Ertan Buyruk
Koray Karabulut

ISSN 1333-1124

NUMERICAL INVESTIGATION INTO HEAT TRANSFER FOR THREE-DIMENSIONAL PLATE FIN HEAT EXCHANGERS WITH FINS PLACED PERPENDICULAR TO FLOW

UDC 536.2:519.6

Summary

In the present study, the potential of rectangular fins with a 30^{o} and 60^{o} angle and 10 mm offset from the horizontal direction perpendicular to flow for heat transfer enhancement in a plate fin heat exchanger is numerically evaluated with the use of a conjugated heat transfer approach. The rectangular fins are mounted on a flat plate channel. Numerical computations are performed by solving a steady, three-dimensional Navier-Stokes equation and an energy equation by using the Fluent software program. The study is carried out at Re=400 inlet temperatures, velocities of cold and hot air are fixed at 300 K, 600 K and 1.338 m/s, 0.69 m/s, respectively. The results show that heat transfer is increased by about 9 % at the exit of the channel with a fin angle of 60^{o} when compared to the channel without fins for parallel flow. The heat transfer enhancement with fins of 30^{o} and 60^{o} for different values of the Reynolds number with 300 and 800 and for varying fin heights, fin intervals and also temperature distributions on the hot and cold fluid sides of the channel outside surface are investigated in the parallel and counter flow arrangement.

Key words: *plate heat exchanger, numerical heat transfer, fin*

1. Introduction

Improvement in the heat transfer process is desired in heat exchangers to enable reductions in weight and size, to increase the heat transfer rate, to diminish the mean temperature difference between the fluids and thus to improve the overall process efficiency. The methods to improve or enhance heat transfer usually involve extended surfaces or some form of surface modification, destabilization of the flow field and generation of a secondary flow [5].

In today's technology, to increase the amount of heat transfer one of the widely used methods is extended heat transfer surfaces. The surfaces with fins raise convective heat and mass transfer by expanding the surface area and raising the current of turbulance. Areas of application of surfaces with fins are very various. The main areas are cooling of gas turbine engines, cooling of turbine blades and electronic devices, some heat exchangers used in chemical plants and airplanes. However, when appropriate fins are not used, heat transfer can be reduced instead of increased. It is necessary to consider each of the fin materials, the fin type, the order of fin placement, assembly methods on the surface and each of environmental conditions and to evaluate them in the way to increase heat transfer. Many theoretical and experimental studies have been carried out to understand heat transfer and flow structures in plate fin heat exchangers. One of the earliest thorough investigations into the heat transfer enhancement was carried out by using expanded surfaces formed by different installations experimentally and numerically in tablet type heat exchangers for laminar and low turbulance flow rates [12]. Numerical heat transfer and the flow form from a horizontal surface for two dimensional ribs with the use of a CFD model were researched by Lee and Abdel-Moneim [8]. Acharya et. al. [1] carried out experimental and numerical flow and heat transfer investigations in the channel having fins for fluid area that improves periodically. Liou, Chang and Hwang [9] and Liou, Hwang [10] investigated different fin heights and flow rates on varied inclinations for two pairs of turbulance supporters arranged one after another in order to improve the channel flow ($1.2x10^4<Re<12x10^4$). Effects on heat transfer of three types of extended surface geometries placed on two dimensional rectangular cross-section flat plate channels were investigated numerically by Kaya D. et. al. [7]. Ganzarolli MM. and Alternai CAC. [3] carried out a study to obtain the optimum fin spacing and thickness according to the minumum inlet temperature difference and the criteria for the minumum number of entrophy generation units for the thermal design of a counter flow heat exchanger with the use of air as a working fluid. Wang YQ. et al. [13] analyzed fluid flow and heat transfer characteristics of plate fin heat exchangers with plain fins and serrated fins. The numerical simulations for heat exchangers with two fins at low Reynolds numbers were carried out by using the CFD code FLUENT. Masliyah and Nandakumar [11] obtained heat transfer characteristics for tubes with triangle fin by using the finite elements method. They concluded that the optimum fin number exists in fin setups for highest heat transfer. Gupta M. et. al. [4] investigated numerically the flow structure and heat transfer performance of the winglet pair type vortex generator in a plate fin heat exchanger with triangular fins by using the MAC method. By varying the heights of the winglet pair, heat transfer enchancement ratio was also predicted. Zhu YH. and Li YZ. [15] investigated numerically the thermal entry and end effect on the flow and heat transfer characteristics for four different types of fins (rectangular plate fin, strip ofset fin, perforated fin and wavy fin) at the laminar flow regime by taking into account fin thickness three dimensionally. Wasewar KL. et al. [14] studied flow distribution through a plate fin heat exchanger by comparing the modified with the conventional heat exchanger by using the CFD code FLUENT.

In this study, the effects of the fins with a 30^o and 60^o angle and 10 mm offset in the horizontal direction perpendicular to the flow on the flow structure and heat transfer enhancement of plate fin heat exchangers have been investigated. Also, the importance of different fin angles, fin heights and fin intervals on heat transfer enhancement were examined numerically. The effect of the Reynolds number on the Nusselt number was also examined both for the paralel and the counter flow. And at the top and bottom surface of the channel, the influence of the different fin angles on the temperature distribution was studied. Calculations were carried out by using the Fluent software program. The results were presented as temperature contours, local temperature and the Nusselt number distribution for different fin angles and flow conditions when compared with the flat channel.

2. Numerical Method

The numerical study has been conducted to study the three-dimensional, steady, conjugate heat transfer of forced convection and conduction in a channel wall. The finite volume method (FLUENT program) was used to solve the conjugate heat transfer analysis.

The finite volume method is based on the principle of dividing the geometry which will be solved in portions to find a solution for each of these sections and then by uniting these solutions to find a general solution to the problem. This method uses a technique which is based on the control volume for transforming heat flow equations into algebraic equations which can be solved numerically. In other words, this technique is based on the principle of taking the heat flow equations integration in each control volume. This integration result provides equations which characterize each control volume which occurs. For preparing the most appropriate grid model, a fine grid should be formed in regions where the change in variables such as velocity, pressure and temperature is bigger. Therefore, the channel surfaces with the fins make the finest grid and in other zones a sparser grid has been preferred. In the numerical model, the channel with fins has included 25000 cells in solid zones and 74000 cells in fluid zones, and the effect of the grid size on the temperature variations was investigated. Convergence of the computations is stopped for the continuity and the momentum equations when residues are less than 10-4 and for the energy equation when residues are less than 10-7. A grid structure which consisted of quadrilaterals was used for simulation.

Since the used fins cause turbulance, it is determined that a standard k-ε turbulance model is appropriate for the selected models with fins in the numerical investigations.

The flow and heat transfer through the geometry are governed by the partial differential equation derived from the laws of conservation of mass, momentum and energy with steady state conditions without a body force, which are expressed as follows [13,2].

-Continuity equation

$$\frac{\partial u}{\partial x}+\frac{\partial v}{\partial y}+\frac{\partial w}{\partial z}=0 \tag{1}$$

-Momentum equation

x momentum equation

$$\rho\left(u\frac{\partial u}{\partial x}+v\frac{\partial u}{\partial y}+w\frac{\partial u}{\partial z}\right)=-\frac{\partial p}{dx}+\mu\left(\frac{\partial^2 u}{\partial x^2}+\frac{\partial^2 u}{\partial y^2}+\frac{\partial^2 u}{\partial z^2}\right) \tag{2.1}$$

y momentum equation

$$\rho\left(u\frac{\partial v}{\partial x}+v\frac{\partial v}{\partial y}+w\frac{\partial v}{\partial z}\right)=-\frac{\partial p}{\partial y}+\mu\left(\frac{\partial^2 v}{\partial x^2}+\frac{\partial^2 v}{\partial y^2}+\frac{\partial^2 v}{\partial z^2}\right) \tag{2.2}$$

z momentum equation

$$\rho\left(u\frac{\partial w}{\partial x}+v\frac{\partial w}{\partial y}+w\frac{\partial w}{\partial z}\right)=-\frac{\partial p}{\partial z}+\mu\left(\frac{\partial^2 w}{\partial x^2}+\frac{\partial^2 w}{\partial y^2}+\frac{\partial^2 w}{\partial z^2}\right) \tag{2.3}$$

Energy equation

$$u\frac{\partial T}{\partial x}+v\frac{\partial T}{\partial y}+w\frac{\partial T}{\partial z}=\left(\frac{k}{\rho c_p}\right)\left(\frac{\partial^2 T}{\partial x^2}+\frac{\partial^2 T}{\partial y^2}+\frac{\partial^2 T}{\partial z^2}\right) \tag{3}$$

In the equations, ρ is density, μ dynamic viscosity, p pressure, k thermal conductivity, T temperature, Cp specific heat and u,v,w are velocities of the x, y and z direction, respectively.

In the used standard $k-\in$ turbulance model, the turbulence kinetic energy k' and its rate of dissipation $\in$, and the viscous disappearance term ϕ are used.

Steady flow turbulence kinetic energy equation

$$\frac{\partial(\rho uk')}{\partial x}+\frac{\partial(\rho vk')}{\partial y}+\frac{\partial(\rho wk')}{\partial z}=\frac{\partial}{\partial x}\left(\frac{\mu_t}{\sigma_k}\frac{\partial k'}{\partial x}\right)+\frac{\partial}{\partial y}\left(\frac{\mu_t}{\sigma_k}\frac{\partial k'}{\partial y}\right)+\frac{\partial}{\partial z}\left(\frac{\mu_t}{\sigma_k}\frac{\partial k'}{\partial z}\right)+\mu_t\phi-\rho\varepsilon \tag{4}$$

Turbulent viscosity

$$\mu_t = C_\mu.\rho.\frac{k'^2}{\varepsilon} \tag{5}$$

Turbulence kinetic energy

$$k' = \frac{1}{2}\left(\overline{u'^2} + \overline{v'^2} + \overline{w'^2}\right) \tag{6}$$

Viscous disappearance term

$$\phi = 2\mu\left[\left(\frac{\partial u}{\partial x}\right)^2 + \left(\frac{\partial v}{\partial y}\right)^2\right] + \mu\left(\frac{\partial v}{\partial x} + \frac{\partial u}{\partial y}\right)^2 \tag{7}$$

Turbulence kinetic energy disappearance equation

$$\frac{\partial(\rho u\varepsilon)}{\partial x} + \frac{\partial(\rho v\varepsilon)}{\partial y} + \frac{\partial(\rho w\varepsilon)}{\partial z} = \frac{\partial}{\partial x}\left(\frac{\mu_t}{\sigma_\varepsilon}\frac{\partial \varepsilon}{\partial x}\right) + \frac{\partial}{\partial y}\left(\frac{\mu_t}{\sigma_\varepsilon}\frac{\partial \varepsilon}{\partial y}\right) + \frac{\partial}{\partial z}\left(\frac{\mu_t}{\sigma_\varepsilon}\frac{\partial \varepsilon}{\partial z}\right) + C_{1\varepsilon}\mu_t\frac{\varepsilon}{k'}\phi - C_{2\varepsilon}\rho\frac{\varepsilon^2}{k'} \tag{8}$$

The model constants C_μ , $C_{1\in}$, $C_{2\in}$, σ_k and σ_ε have default values as follows;

C_μ =0.09, $C_{1\varepsilon}$ = 1.44, $C_{2\varepsilon}$ = 1.92, σ_k = 1 and σ_ε = 1.3.

Reynolds number is calculated with

$$\mathrm{Re} = \frac{V_\infty \cdot d}{v} \tag{9}$$

Here, *d* is the hydraulic diameter of the duct.

The Nusselt number is evaluated as the conductive heat transfer rate of the fluid over the solid boundary equals its convective heat rate as:

$$-k\left(\frac{dT}{dn}\right)_{surface} = h\left(T_\infty - T_s\right) \text{ and } Nu = \frac{h.d}{k},\ h = \frac{-k_f \left.\frac{\partial T}{\partial y}\right|_{y=0}}{T_s - T_\infty} \tag{10}$$

Where *h* is the local heat transfer coefficient on the surface and the local Nusselt number is obtained as above.

Here, $\left.\frac{\partial T}{\partial y}\right|_{y=0}$ is the temperature gradient on the channel surface and k_f indicates fluid thermal conductivity.

As thermal conductivity of a fin material affects heat distribution along the fin, the selection of the fin material is an important factor for the enhancement of heat transfer. Therefore, aluminum, which has high thermal conductivity and is cheap and light, has been chosen as the channel material. By assuming that fins have been produced together with the channel surface as a whole, the thermal contact resistance between the fins and the surface was neglected.

3. Geometric Model

While Fig. 1 shows perspective view of the models, Fig. 2a and Fig. 2b point out the computational models that were used in the present study for rectangular channels with the fin angle of 30^o and 60^o, respectively. The boundary conditions can also be seen in these figures. Channels are reversed to show fins in Fig. 2a and Fig. 2b.

The variables used in the models are taken as follows:

$e = 2$ mm, 4 mm, $b = 20$ mm, 60 mm, $p = 3$ mm, $\Phi = 30^o$ and 60^o,

L= 300 mm, W=150 mm,

H_1= 5 mm, H_2= 10 mm, t=2 mm, Re= 300, 400, 800, Th= 600 K,

Tc=300 K, V_h= 0,69 m/s,

V_c= 1,338 m/s. Also, the fin shape is rectangular for all the models.

In the present study, numerical results are presented for the Reynolds number of 400 in order to see the effects of fins on heat transfer at low velocities. The effect of different Reynolds numbers is also investigated with the values of 300 and 800. 12 fins with are placed on the flat plate channel at an equal interval. When the distance between two fins is 20 mm, there is 25 mm space between the entry section of the channel and the first fin. In order to increase turbulance, fins are placed with a 10 mm offset from the horizontal direction perpendicular to the flow.

The study is conducted under the following assumptions:

i) The flow field is assumed to be three-dimensional, steady-state and laminar for flat channel;

ii) Calculations are carried out for incompressible fluid;

iii) Aluminum's thermal conductivity is chosen as 202.4 W/(m.K);

iv) There is a perfect thermal contact between fins and base surface;

v) Air is used as working fluid for the top and bottom section of the duct;

vi) Thermal properties of the fluid are constant;

vii) There is no heat generation for both the fluid and the solid materials.

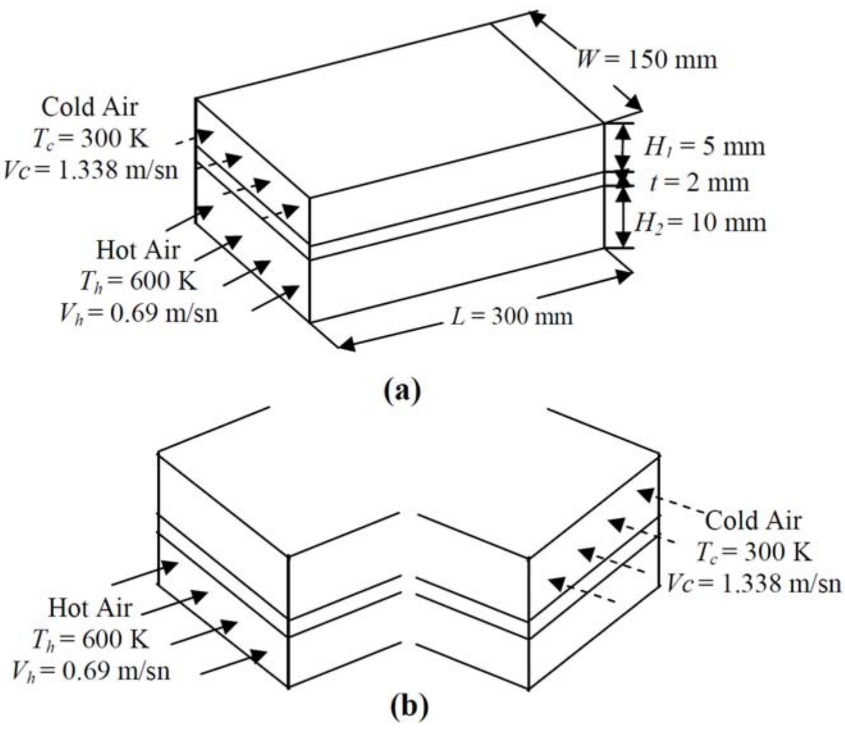

Fig. 1 Perspective views of models of flat channels **(a)** paralel flow **(b)** counter flow

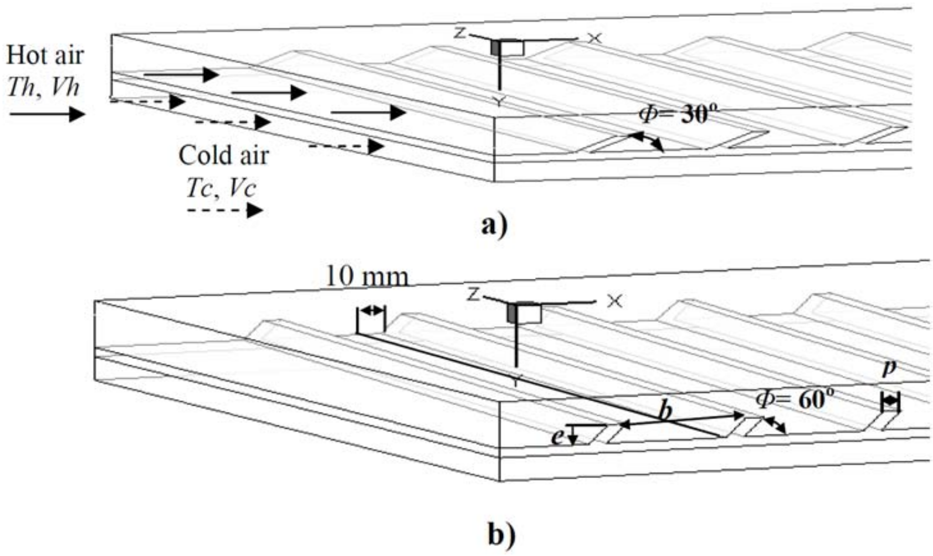

Fig. 2 Computational models of flat channels with 30^0 and 60^0 fin angle in paralel flow arrangement **a)** Φ= 30°, b= 20 mm, e= 4 mm, **b)** Φ= 60°, b= 20 mm, e= 4 mm

4. **Evaluation of the Results**

Figure 3 presents a comparison of the present study with the study performed by Kayatas N. and Ilbas M. [6]. It can be seen that the results are well comparable and the numerical model is reasonable and appropriate. It is considered that there is a small temperature difference between the fluids due to the mesh structure.

To determine the effect of the grid size on the temperature variations, a grid independence test (as shown in Fig. 4) was performed for the channel with the fin angle of 30°. The test indicates that 99000 grids (25000 grids in the solid zones and 74000 grids in the fluid zones) on the duct cross-section are adequate (< 0.1% difference compared with 110000 grids).

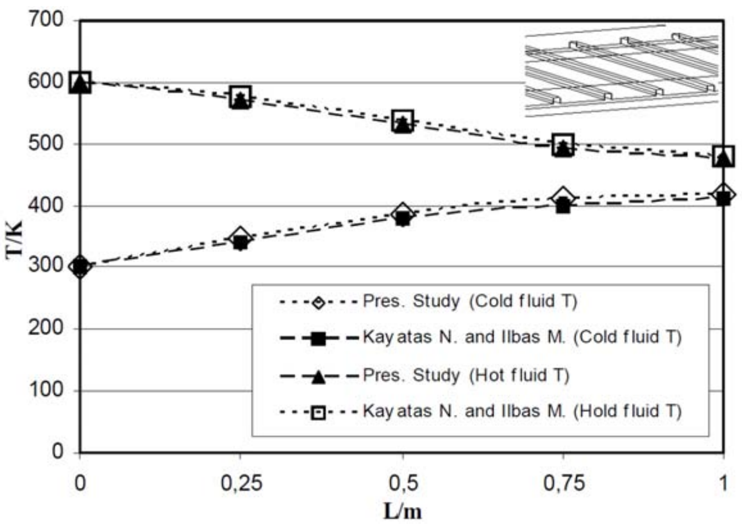

Fig. 3 Comparison of the presented study with the study by Kayatas N. and Ilbas M. on channel with fins

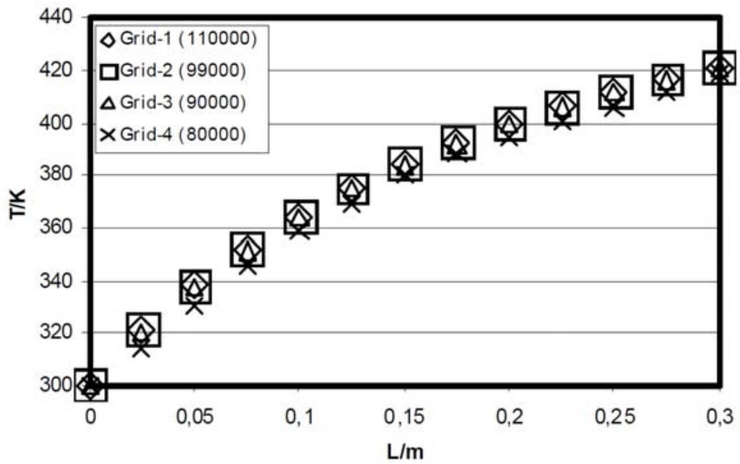

Fig. 4 Grid independence of results for cold fluid along the channel with fin angle of 30^o

The temperature distribution for the three-dimensional channel without fins and with fins having a 30^o and 60^o angle and 10 mm offset from the horizontal direction perpendicular to the flow are shown in Fig. 5a and Fig. 5b in the parallel and counter flow arrangement, respectively. In the parallel flow arrangement, while the heat transfer rate is high at the inlet section of the duct, heat transfer decreases as the temperature difference between hot and cold fluids decreases along the channel but it continues to increase in the counter flow arrangement. Thus, the temperature contour gradient of the counter flow is higher than that of the parallel flow for both hot and cold fluids (Fig. 5a and Fig. 5b). However, as shown in Fig. 5a, at the fin angle of 30^o the temperature gradient of the cold fluid is determined to be higher than that of the angle of 60^o along the channel for each of two flow types as expected. The reason of this enhancement can be explained with a larger heat transfer surface area and the increased turbulance effect of the flow. . In conclusion, it is observed that higher hot fluid temperature variation for the channel with the fin angle of 30^o is obtained compared with the angle of 60^o as indicated in Fig. 5b. Furthermore, it can be clearly seen that the temperature contour variation of the channel with the fin angles of 30^o and 60^o is more changeable than the flat channel.

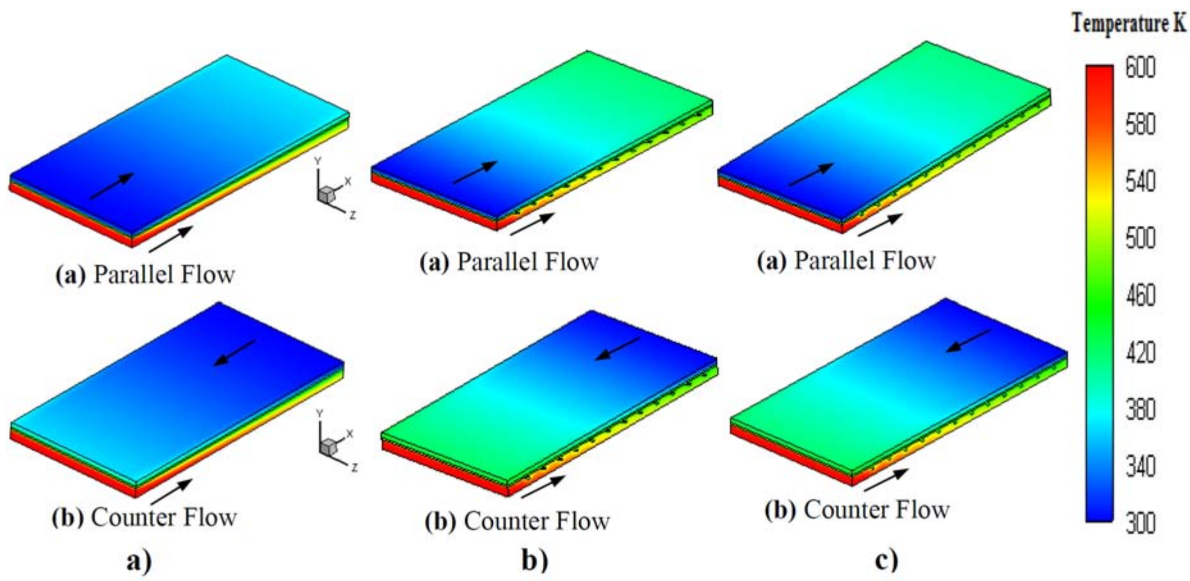

Fig. 5a Three-dimensional temperature distribution of cold fluids
a) flat channel **b)** Φ= 30^o **c)** Φ= 60^o (b=20 mm, e=4 mm)

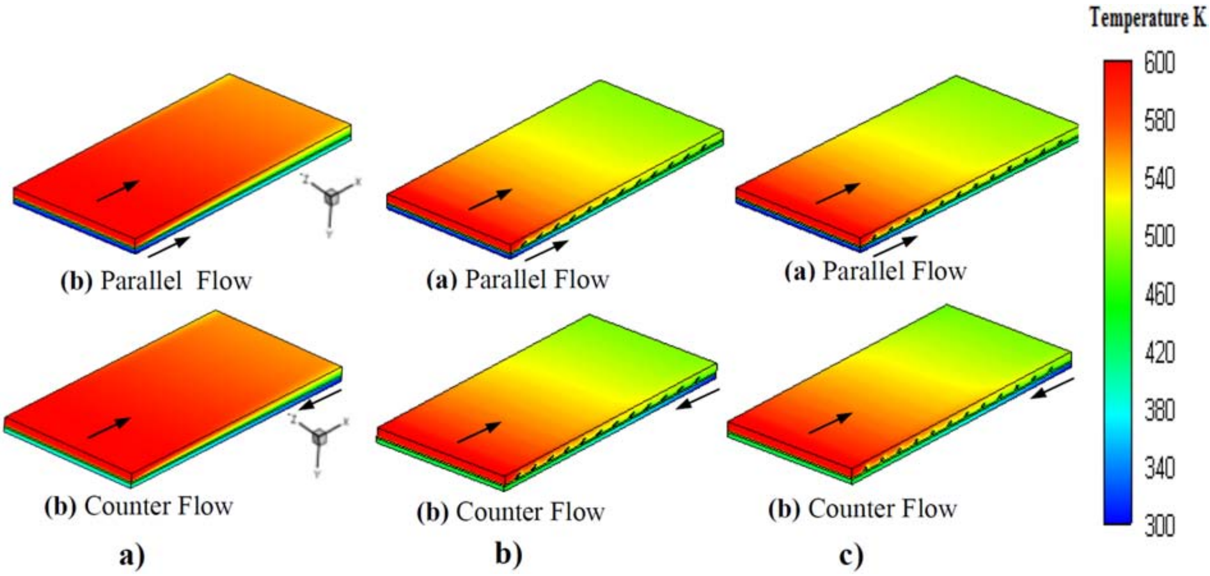

Fig. 5b Three-dimensional temperature distribution of hot fluids
a) flat channel **b)** Φ= 30^o **c)** Φ= 60^o (b=20 mm, e=4 mm)

In Figs. 6a and 6b, the temperature distributions with velocity streamlines at the inlet section of the channel with the fin angles of 30^o and 60^o are given for the parallel flow. The increased surface area within the hot fluid raises the turbulance effect behind the fins. Therefore, currents of turbulance for the fin angle of 30^o which has a larger heat transfer surface area are higher than that of the angle of 60^o. So, this case leads to a higher heat transfer rate obtained in the case of the 30^o fin angle for the same fin height.

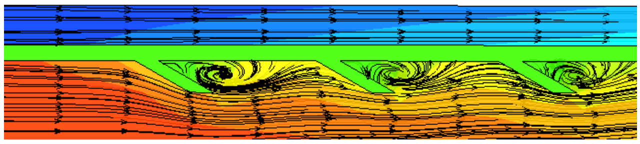

Fig. 6a Temperature distribution with velocity streamlines for channel with 30^o fin angle

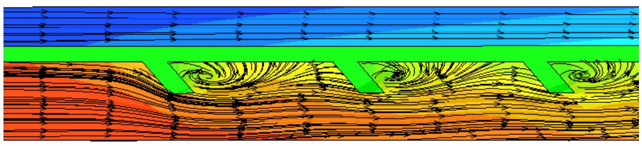

Fig. 6b Temperature distribution with velocity streamlines for channel with 60^o fin angle

Temperature variations of the cold fluid along the middle section of the channel with fin angles of 30^o and 60^o for the parallel and counter flow are shown in Fig. 7a and Fig. 7b, respectively. Fins have an important effect which is produced when the surface area and turbulance of the flow are increased. Therefore, it is observed that the heat transfer rate from the hot fluid to the cold fluid increases. As seen in Fig. 7a, when compared to the cold fluid inlet temperature, the outlet temperature increases up to 41 % for the parallel flow with the fin angle of 30^o, while this value raises to 38.5 % for the fin angle of 60^o under the same conditions. As it is shown in Fig. 7b, the outlet temperature difference of the cold fluid for the 30^o fin angle goes up to 4 K compared with the angle of 60^o in the counter flow arrangement. Meanwhile, the temperature increases up to 10 % at the exit of the channel with the fin angle of 30^o compared to the channel without the fins for the counter flow. These results indicate that under the counter flow enhancement the rate of the temperature is higher than that of the parallel flow along the channel. Therefore, in Fig. 7b the temperature line is more linear than in Fig. 7a.

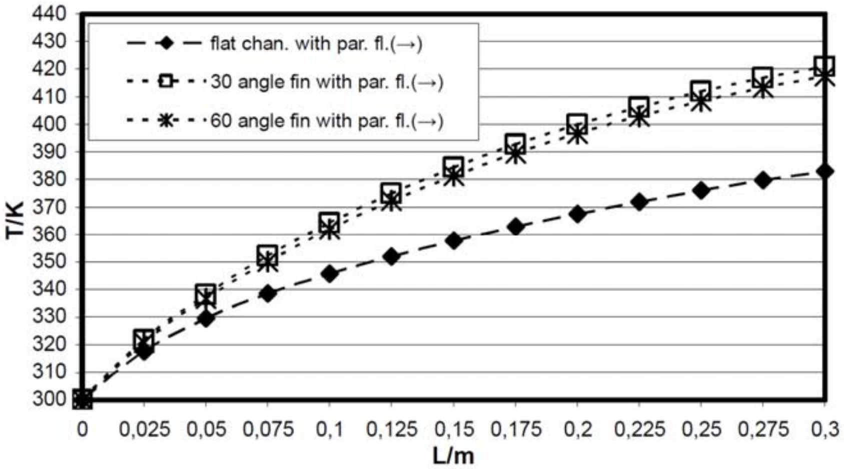

Fig. 7a Cold fluid temperature variations for flat channel, Φ= 30° and 60° in parallel flow arrangement (b= 20 mm, e= 4 mm)

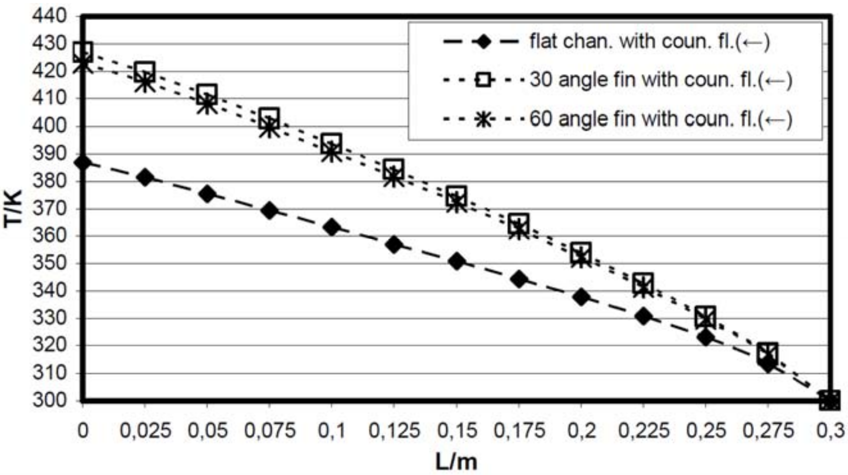

Fig. 7b Cold fluid temperature variations for flat channel, Φ= 30° and 60° in counter flow arrangement (b= 20 mm, e= 4 mm)

Because the purpose of this study is to investigate the effect of fins placed on the hot fluid side of the channel on heat transfer performance of the cold fluid, variations of the local Nusselt number and the temperature at different Re numbers along the channel solid surface, which is closed for the hot fluid in the plate fin heat exchangers with fin angles of 30° and 60° in the parallel flow arrangement, are given in Fig. 8a and Fig. 8b, respectively. It is observed that by increasing the fluid velocity, the improvement in heat transfer increases. The effective parameters on the heat transfer coefficient can be listed as velocity (Re number), turbulance, which is caused by the fins, and the temperature difference between fluids. However, since the local temperature difference between the hot and the cold fluid decreases towards the exit of the channel for the Reynolds number analyzed, the heat transfer rate and the local heat transfer coefficient decrease in the parallel flow. As a result, the values of the local Nu number decrease continuously from the inlet to the outlet of the channel. When the maximum Nu number value with Re=800 for the 30° fin angle is reached, the minimum local Nu number value is obtained in the case of the angle of 60° with Re=300. As it can be seen in Fig. 8b, it is determined that there is about 7 K temperature difference between the Reynolds number values of 800 and 300 in the case of the angle of 30° at the distance of 0.275 m from the channel entrance. Also, measurement points are shown with an arrow on the model on graphics.

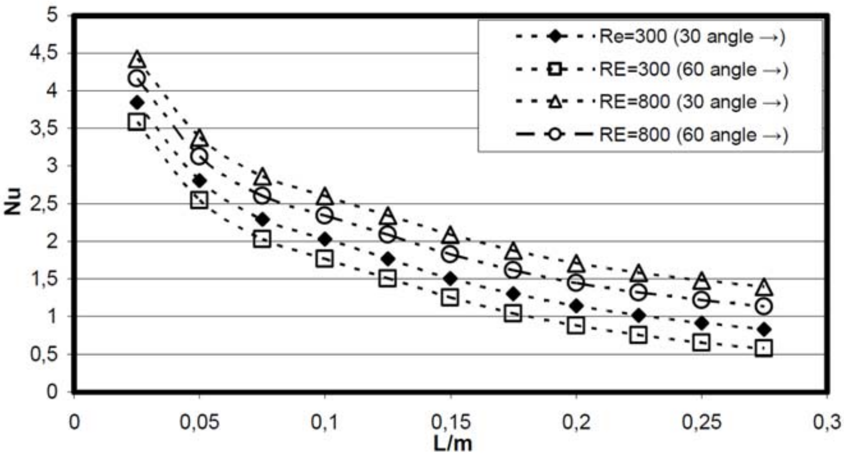

Fig. 8a Local Nusselt number variation with different *Re* numbers and fin angles on channel surface of cold fluid in parallel flow arrangement (*b*= 20 mm, *e*= 4 mm)

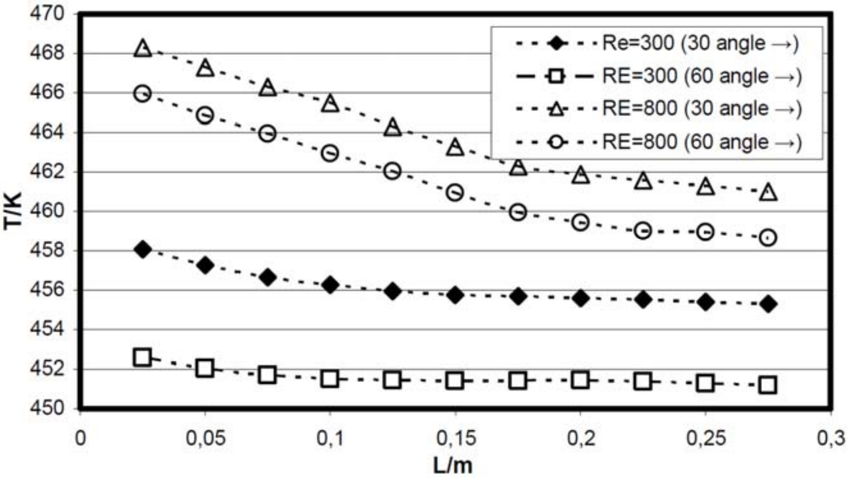

Fig. 8b Temperature variation with different *Re* numbers and fin angles on channel surface of cold fluid in parallel flow arrangement (*b*= 20 mm, *e*= 4 mm)

In Fig. 9a and Fig. 9b, the local Nusselt number and temperature variations for the cold fluid at different Re numbers along the channel solid surface close to the hot fluid in the counter flow arrangement are shown for the plate fin heat exchangers with fin angles of 30^o and 60^o, respectively. As it is seen in Fig. 9a, because the fluid warms up towards the entry section of the channel for all the Re numbers and fin angles, the heat transfer rate goes down. Therefore, the local Nusselt number values are higher at the exit of the channel in the counter flow arrangement. Meanwhile, over the range studied, the maximum local Nu number values are found with the use of the 30^o fin angle at the Reynolds number of 800. The temperature value of the cold fluid increases up to about 2.5 % for the distance of 0.025 m from the entrance of the channel with the fin angle of 60^o at *Re*=800 compared to *Re*=300 with the same distance and the fin angle (Fig. 9b). As all the Reynolds numbers are analyzed, it is possible to say that the value of temperature and the Nusselt number increase as the Reynolds number increases and the effect of the fin angle of 30^o on heat performance of the plate fin heat exchanger is stronger than that of the angle of 60^o.

The effect of different fin heights with a fin angle of 60^o on the temperature variation of the hot fluid through the middle of the channel in the parallel and counter flow arrangement is shown in Figure 10. An increase in the height of the fin leads to an increase in the heat transfer surface area, which results in an increase in the heat transfer rate and a decrease in the hot fluid temperature.

The temperature distributions contours on the top and bottom channel surface are given in Figs. 11a and 11b for fin angles of 30^0 and 60^0 in the parallel and counter flow arrangement, respectively. The contour distributions do not show temperatures of hot and cold fluids, they are surface temperatures of the channel caused by hot and cold fluids and show high temperature variations at small distances along the channel thanks to the fins. As it is seen from Figs. 11a and 11b, when compared with the case of the angle of 60^o, the variation of the temperature occurs earlier and a higher temperature gradient appears where heat transfer is more efficient both for the parallel and counter flow at the fin angle of 30^o. However, it is understood from the distribution of temperature that the efficiency of the counter flow is higher for each of the two fin angles due to the larger temperature gradient along the channel. Also, on the contour distributions, the flow directions are displayed with arrows for the parallel and counter flow.

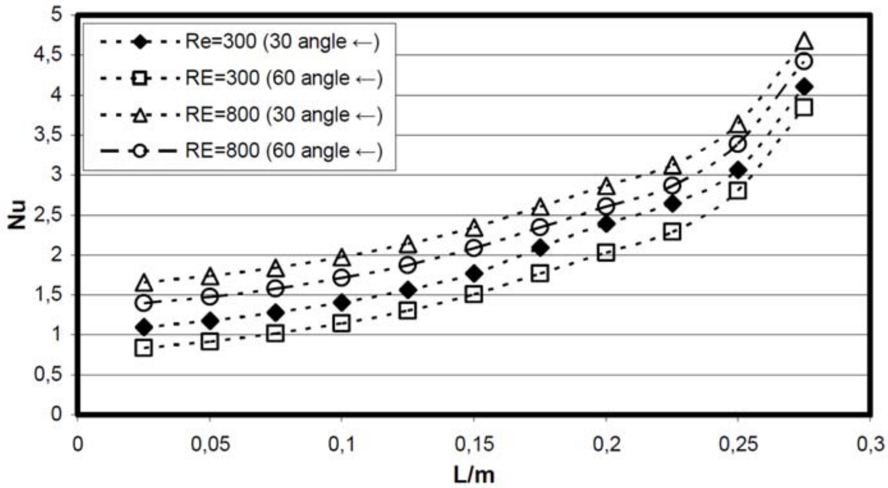

Fig. 9a Local Nusselt number variation with different *Re* numbers and fin angles on channel surface of cold fluid in counter flow arrangement (*b*= 20 mm, *e*= 4 mm)

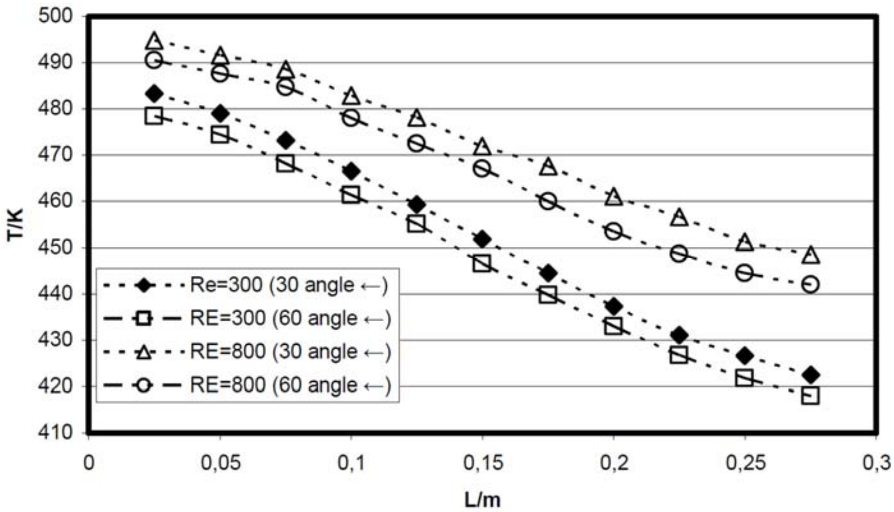

Fig. 9b Temperature variation with different *Re* numbers and fin angles on channel surface of cold fluid in counter flow arrangement (*b*= 20 mm, *e*= 4 mm)

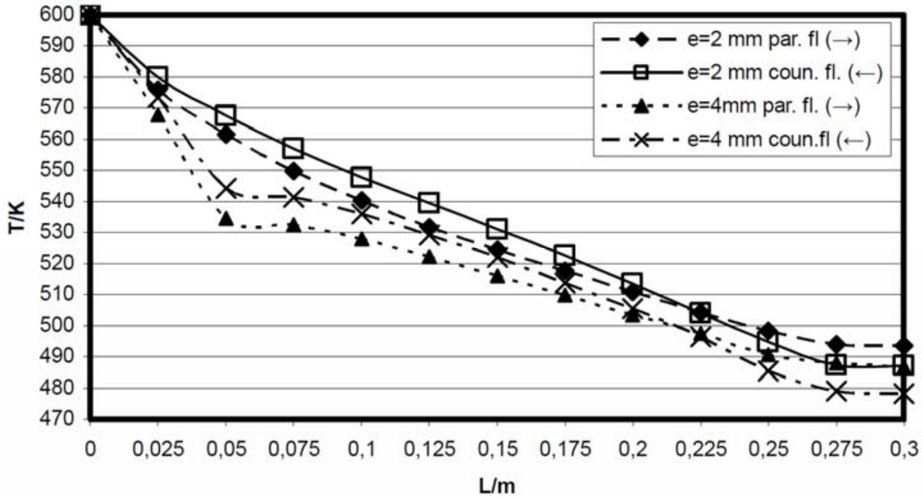

Fig. 10 Temperature variation of hot fluid in parallel and counter flow arrangement for e= 2 and 4 mm fin heights at Φ= 60°

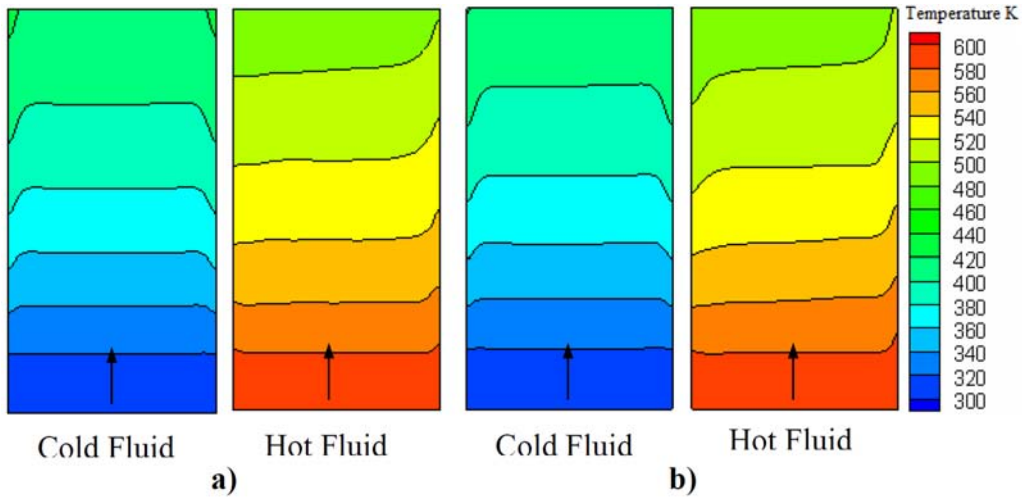

Fig. 11a Temperature distribution of fluid for parallel flow **a)** Φ= 30° and **b)** Φ= 60°

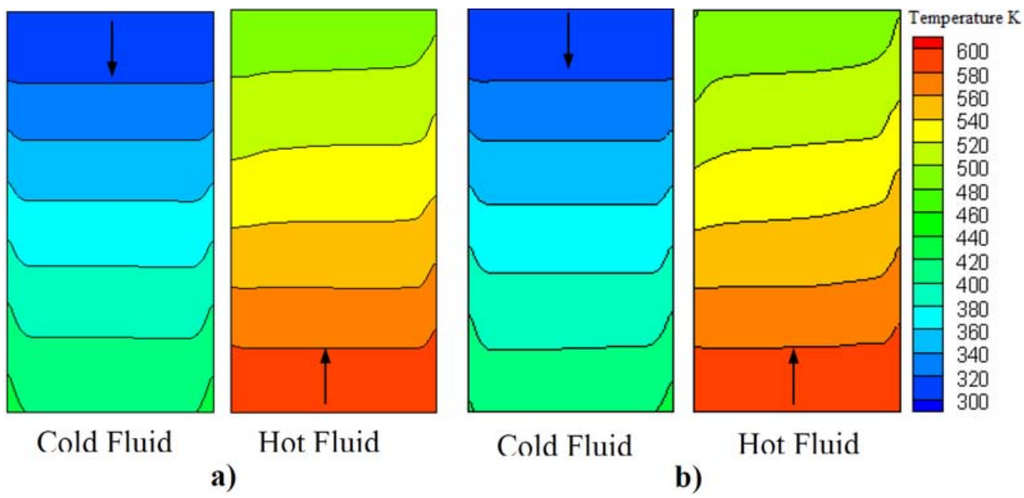

Fig. 11b Temperature distribution of fluid for counter flow a) Φ= 30° and b) Φ= 60°

Temperature variations of the duct top surface for the cold fluid on the channel without fins and with the fin angles of 30° and 60° are shown in Fig. 12. While the first temperature variation from the entry section of the flat channel improves at 0.10671 m, it develops at

0.04395 m for the channel with the fin angle of 30^o in the parallel flow arrangement. For the counter flow, similar results can be seen in Fig. 12. It is concluded that by adding fins to the channel surface the turbulance develops earlier and the heat transfer surface area increases. Meanwhile, the temperature values of the cold fluid for the case of the angle of 30^o are higher compared to the fin angle of 60^o**.**

The effect of different fin interval values of 20 mm and 60 mm on the variation of the cold fluid temperature along the middle of the channel with the fin angle of 60^o and the fin height of *e*=4 mm are shown in Figs. 13a and 13b in the parallel and the counter flow arrangement, respectively. When the fin interval is increased, the number of fins on the channel decreases and so both the heat transfer surface area and the effect of the turbulance caused by fins reduce. As seen in Fig. 13a, the cold fluid temperature for the fin interval of *b*=20 mm is higher than for the fin interval of *b*=60 mm along the channel in the parallel flow arrangement. Although a similar case is also obtained for the counter flow (Fig. 13b), higher outlet fluid temperature values are determined when compared to the parallel flow.

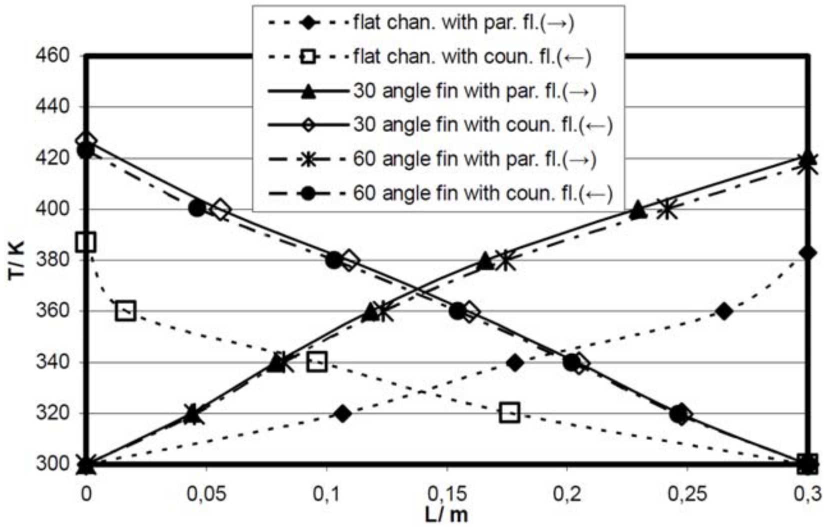

Fig. 12 Temperature variation of cold fluid on channel surface without fins and with fin angles of 30^o and 60^o for parallel and counter flow (*b*= 20 mm, *e*= 4 mm)

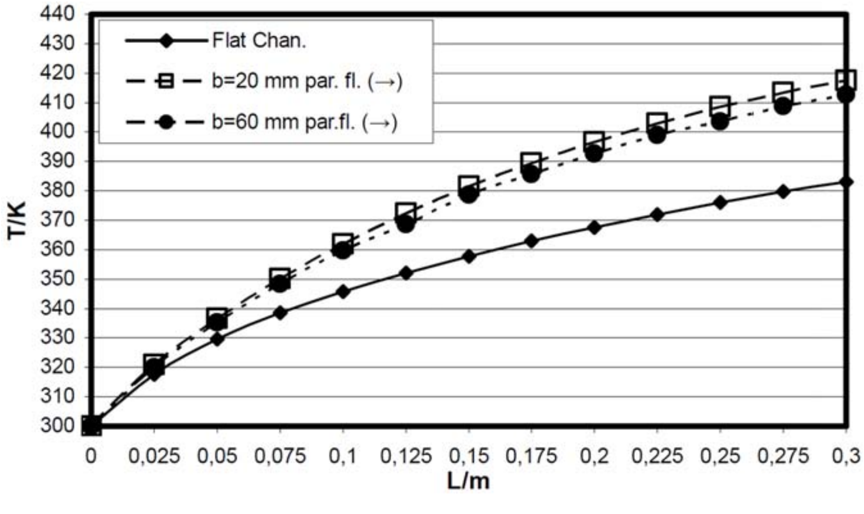

Fig. 13a Temperature variation of cold fluid with parallel flow for *b*=20 and 60 mm fin interval with e=4 mm at Φ= 60^o

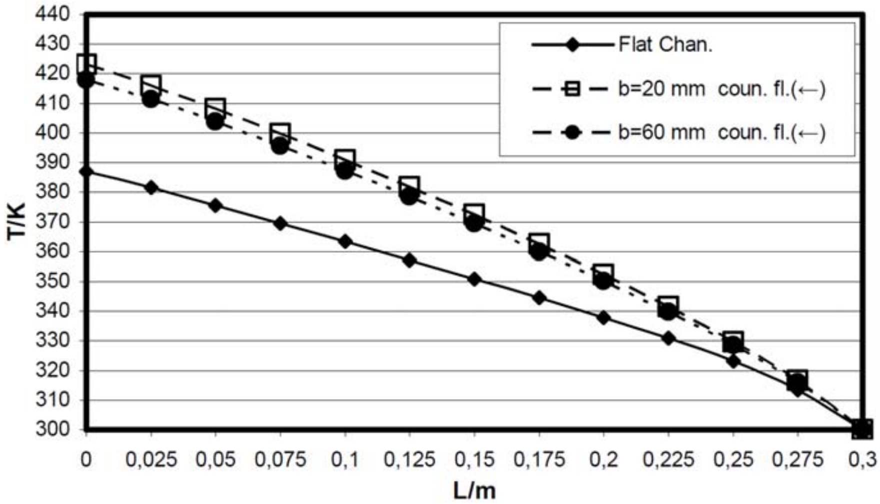

Fig. 13b Temperature variation of cold fluid with counter flow
for b=20 and 60 mm fin interval with e=4 mm at Φ= 60^{o}

5. **Conclusions**

The characteristics of the fluid flow and heat transfer in the three-dimensional plate fin heat exchangers with rectangular fins with a 30^{o} and 60^{o} angle and 10 mm offset from the horizontal direction perpendicular to the flow are carefully investigated in this study, in which the effects of the fin height, the fin interval, the temperature distributions contours on the top and bottom surface of the channel are also taken into account. Simulations are carried out by using the Fluent packaged sofware program. In this study, the results of the Reynolds number with the value of 400 are presented to see the effect of the use of fins at low velocities on heat transfer. To avoid the high pressure drop and pumping power for the fluid, the low velocity flow is often applied. Further, this study has not included a pressure drop analysis; rather it has focused on the heat transfer performance characteristics of the plate fin heat exchangers with different fin angles. However, the effects of the different Reynolds numbers on the Nusselt number have been examined. An increase in the Re number leads to an increase in the Nu number. When all fin intervals are considered, the optimum result is found to be for the 20 mm fin interval. In any case, the fin angle of 30^{o} for the parallel and the counter flow arrangement shows the best heat transfer rate for both fin heights. The results show that heat transfer is increased by about 9 % at the exit of the channel with the fin angle of 60^{o} when compared to the channel without fins for the parallel flow.

The investigations described in this paper have the goal to increase the efficiency of plate fin heat exchangers by optimizing fin angles, fin intervals and fin heights, offsetting fins along the horizontal direction perpendicular to the flow. The results were presented as temperature contours, the local temperature and the Nusselt number distribution for different fin angles and flow conditions by comparing the channels with fins with the flat channel. Finally, it is considered that this study is of great significance with respect to the design aspect of plate fin heat exchangers in direct applications.

Nomenclature

p	: fin width (mm)	c_p	: specific heat (J/kg K)
b	: fin interval (mm)	p	: pressure (N/m^2)
Φ	: fin angle (^{o})	T	: temperature (K)
e	: fin height (mm)	ν	: kinematic viscosity (m^2/s)
H	: height of channel (mm)	u, v, w	: velocity components of x,y,z directions (m/s)
L	: length of channel (mm)	μ	: dynamic viscosity (kg/s m)
t	: solid surface thickness of channel between fluids (mm)	Re	: Reynolds number
W	: width of channel (mm)	Nu	: Nusselt number
d	: hydraulic diameter (m)	ϕ	: viscous disappearance term
h	: heat transfer coefficient (W/m^2)	u',v',w'	: fluctuating velocity components in x,y,z directions (m/s)
k	: thermal conductivity (W/m K)	μ_t	: turbulent viscosity (kg/sm)
V	: inlet velocity to channel (m/s)	k'	: turbulence kinetic energy (m^2/s^2)
ρ	: density (kg/m^3)	ε	: turbulent dissipation rate (m^2/s^3)

Subscripts

S	:surface	h	:hot	1	:top	f	:fluid
∞	:ambient	c	:cold	2	:bottom		

REFERENCES

[1] S. Acharya, S. Dutta, T.A. Myrum, R.S. Baker: *Periodically Developed Flow And Heat Transfer In A Ribbed Duct*. Int J Heat Mass Transfer. **36**, 2069-2082 (1993).

[2] FLUENT User's Guide: *Fluent Inc*. Lebanon (2003), NH.

[3] M.M. Ganzarolli, C.A.C. Altemani: Optimum Fins Spacing And Thickness Of A Finned Heat Exchanger Plate. Heat Transfer Eng. **31**, 25-32 (2010).

[4] M. Gupta, K.S. Kasana, R. Vasudevan: A Numerical Study Of The Effect Of Flow Structure And Heat Transfer Of A Rectangular Winglet Pair In A Plate Fin Heat Exchangers. J. Mech. Eng. Science. **223**, 2109-2215 (2009).

[5] S. Kakac, A.E. Bergles, F. Mayinger and H. Yüncü: *Heat Transfer Enhancement Of Heat Exchangers*. Kluwer Academic Publischers, Netherlands 1999, pp. 123-140.

[6] N. Kayatas, M. Ilbas: *Iç Içe Borulu Model Bir Isı Değiştiricisinde Isı Transferinin Iyileştirilmesinin Sayısal Olarak Incelenmesi*. Erciyes Universitesi Fen Bilimleri Enstitüsü Dergisi. 21, 128-139 (2005).

[7] D. Kaya, E. Buyruk, A. Can and A. Fertelli: *Numerical Study Of Heat Transfer Characteristics Of Extended Surfaces*. Strojarstvo. **49**, 137-144 (2007).

[8] C.K. Lee, S.A. Abdel-Moneim: *Computational Analysis Of Heat Transfer In Turbulent Flow Past A Horizontal Surface With Two-Dimensional Ribs*. Int Comm Heat Mass Transfer. **28**,161-170 (2001).

[9] T.M. Liou, Y. Chang, D.W. Hwang: *Experimental And Computational Study Of Turbulent Flows In A Channel With Two Pairs Of Turbulence Promoters In Tandem*. ASME J Fluids Eng. **112**, 302-310 (1990).

[10] T.M. Liou, J.J. Hwang: *Developing Heat Transfer And Friction In A Ribbed Rectengular Duct With Flow Seperation At Inlet*. ASME J Fluids Eng. **114**, 565-573 (1992).

[11] J.H. Masliyah, K. Nandakumar: *Heat Transfer In Internally Finned Tubes*. Trans. ASME J Heat Transfer. **98**, 257-261 (1976).

[12] R. Tauscher, F. Mayinger: *Heat Transfer Enchancement In A Plate Heat Exchanger With Rib-Roughened Surfaces*. Heat Transfer Enhancement Of Heat Exchangers. **355**, 207-221 (1999).

[13] Y.Q. Wang, Q.W. Dong, M.S. Liu, D. Wang: *Numerical Study On Plate Fin Heat Exchangers With Plain Fins And Serrated Fins At Low Reynolds Number*. Chem Eng &Tec. **32**, 1219-1226 (2009).

[14] K.L. Wasewar, S. Hargunai, P. Atluri, N. Kumar: *CFD Simulation Of Flow Distribution In The Header Of Plate Fin Heat Exchangers*. Chem. Eng. & Tech. **30**, 1340-1346 (2007).

[15] Y.H. Zhu, Y.Z. Li: *Three Dimensional Numerical Investigation On The Laminar Flow And Heat Transfer In Four Basic Fins Of Plate Fin Heat Exchangers*. Trans. ASME J. Heat Transfer. **130**, 1-8 (2008).

Submitted: 11.9.2012

Accepted: 16.5.2013

Ertan Buyruk
Cumhuriyet Univ.Eng. Faculty,
Mechanical Eng. Dept.
58140 Sivas, Turkey

Koray Karabulut
Cumhuriyet Univ.
Tech. Education Faculty,
Mechanical Dept.
58140 Sivas, Turkey